Universality Classes of Magnetic Domain Wall Motion

Jae-Chul Lee,[1,2] Kab-Jin Kim,[1,*] Jisu Ryu,[3] Kyoung-Woong Moon,[1] Sang-Jun Yun,[1] Gi-Hong Gim,[1] Kang-Soo Lee,[1] Kyung-Ho Shin,[2] Hyun-Woo Lee,[3,†] and Sug-Bong Choe[1,‡]

[1]*CSO and Department of Physics, Seoul National University, Seoul 151-742, Republic of Korea*
[2]*Spin Device Research Center, Korea Institute of Science and Technology, Seoul 136-791, Republic of Korea*
[3]*PCTP and Department of Physics, Pohang University of Science and Technology, Pohang, Kyungbuk 790-784, Korea*
(Received 6 April 2011; published 1 August 2011)

We examine magnetic domain wall motion in metallic nanowires Pt-Co-Pt. Regardless of whether the motion is driven by either magnetic fields or current, all experimental data fall onto a single universal curve in the creep regime, implying that both the motions belong to the same universality class. This result is in contrast to the report on magnetic semiconductor (Ga,Mn)As exhibiting two different universality classes. Our finding signals the possible existence of yet other universality classes which go beyond the present understanding of the statistical mechanics of driven interfaces.

DOI: 10.1103/PhysRevLett.107.067201 PACS numbers: 75.76.+j, 68.35.Rh, 75.78.Fg

Power-law scaling behaviors are abundant in nature [1–5]. Interestingly diverse systems often share the same scaling exponents, implying that the core mechanism is the same despite apparent differences between systems. Additionally, apparently similar systems may exhibit different scaling exponents, signaling that their dynamics are qualitatively different. Thus, scaling exponents allow classification of many phenomena into a small number of universality classes with the same core dynamics.

Magnetic domain wall (DW) motion is a paradigm of scaling behaviors in driven interface dynamics [6–11]. For a small driving force f, the effective energy barrier of the DW motion scales as a power law $f^{-\mu}$ with the creep exponent μ. Theories predict different universality classes depending on the nature of disorders in systems: random-bond (random-field) universality class when disorder potentials (disorder forces) are short-range correlated. Experiments on field-induced DW motion (FIDWM) driven by a magnetic field H ($f = H$) found $\mu \approx 1/4$ and 1.2 for metallic ferromagnet Pt-Co-Pt [8] and ferromagnetic semiconductor (Ga,Mn)As [10] thin films, respectively, and they are attributed to the random-bond and random-field universality classes, respectively.

Spin transfer torque (STT) is an alternative way to induce the DW motion [12,13]. Conduction electrons transfer spin angular momentum to local magnetization, thereby generating this STT proportional to a current density J and inducing the DW motion ($f \propto J$). The STT has two mutually orthogonal vector components, the adiabatic [12] and nonadiabatic STTs [13]. The latter has similar properties as the field-induced torque, and thus, the current-induced DW motion (CIDWM) is expected to have the same exponent [14] as the FIDWM if the nonadiabatic STT is dominant over the adiabatic STT. However, the experiments for (Ga,Mn)As [10] found the exponent $\mu \approx 1/3$ for the CIDWM, different from the FIDWM exponent 1.2 for the material. Thus, Ref. [10] concluded the adiabatic STT to be dominant. This is in contrast to theoretical predictions [15] in ideal systems without disorders and also to experiments [16] for metallic ferromagnets in the large J (flow) regime, both of which indicate that the nonadiabatic STT is the main driving force of the CIDWM.

This raises a number of intriguing possibilities about the relative importance of two STTs for CIDWM: (i) it differs in clean and disordered systems, (ii) it differs depending on the nature of the disorders, or (iii) it differs between small J (creep) and large J (flow) regimes. In this Letter, we report experimental data for the DW motion in a metallic ferromagnet Pt-Co-Pt thin film, which gives insight into the possibilities.

For this study, metallic Pt-Co-Pt films with the Curie temperature far above the room temperature are used. These films exhibit clear circular domain expansion under a magnetic field as low as a few tenths of mT, which implies weak disorders in these films [6]. Several nanowires are patterned with different widths ranging from 190 to 470 nm. Here we show results from the 280-nm-wide nanowire only, except when specified otherwise. Results from the others are basically the same. For the DW speed V measurements, a DW is first created by the local Oersted field in the vicinity of a transverse current line between the function generator (FG1) and the oscilloscope (OSC) in Fig. 1(a) and then pushed to a side by applying H and/or J. The DW arrival time at the other end of the nanowire (red circle) is measured by the magneto-optical Kerr effect (MOKE) signal [6].

Since the pure CIDWM requires a more careful analysis, below we start from the pure FIDWM and move on to the pure CIDWM step by step. The FIDWM is a useful reference to characterize our sample. It follows [Fig. 1(b)] the well-known creep scaling behavior for metallic ferromagnets, $V(H) = V_0 \exp(-\alpha H^{-\mu}/k_B T)$ with the exponent $\mu = 1/4$ [8,9]. Note that the DW speed V follows the

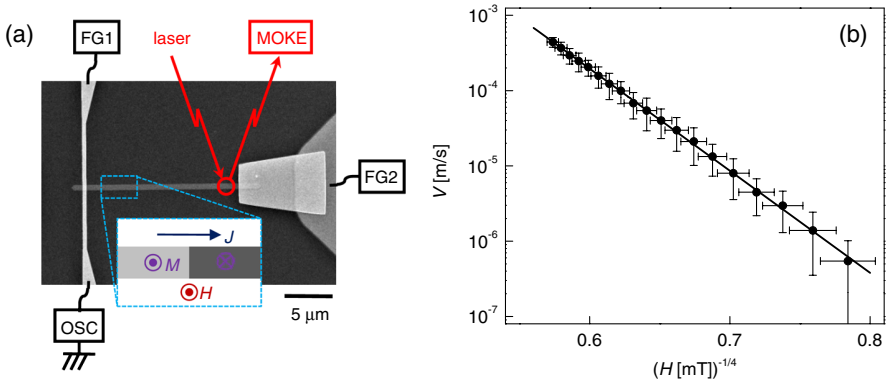

FIG. 1 (color online). (a) Secondary electron microscope image for a nanowire with schematic drawing of measurement setup. The definition of the positive polarities of J, H, and the magnetization M is shown in the inset. (b) Scaling behaviors of the pure FIDWM. The line shows the best linear fit.

Arrhenius law with the effective energy barrier $\alpha H^{-\mu}$ [8,9] and the thermal energy $k_B T$. Here, α is a scaling constant and V_0 is the characteristic speed.

Next, we examine effects of J on the FIDWM. To compensate for the Joule heating effect, we convert V measured at the elevated temperature $T(J)$ to V^* at the constant ambient temperature $T_0 \equiv T(J = 0)$, based on the Arrhenius law [17,18] combined with $T(J)$-dependent electric resistance measurement [19]. The resulting V^* is depicted in Fig. 2(a). Note that $+J$ and $-J$ induce parallel shifts of the pure FIDWM curve (dotted line) in the opposite directions.

Figure 2(b) shows a 2D contour map of V^* as a function of H and J. The color scale represents the magnitude of V^*. Each color contrast thus visualizes "equispeed" contours. For a quantitative analysis, H is measured as a function of J for several equispeed contour lines and plotted onto the map (symbols with error bars). We find that each contour line is well fitted by a quadratic function of J, $H(J) = H^* + \varepsilon J + cJ^2$. Here H^* is the value of the magnetic field for each contour line at $J = 0$. Combined with the creep scaling formula for the case $H = H^*$ and $J = 0$, the equispeed contour lines in the (H, J) plane completely specify the DW speed. It is thus important to understand the equispeed contour lines.

The linear term εJ is the leading order contribution of J to the FIDWM and captures the fieldlike effect of the STT. If the quadratic term cJ^2 was negligible, it implies that J affects the FIDWM mainly through the nonadiabatic STT. By the way, regardless of the quadratic term issue, ε can be determined from the horizontal spacing between the curves for $\pm J$ in Fig. 2(a), which, for fixed V^*, amounts to $2\Delta H_1(J) \equiv H(J) - H(-J) = 2\varepsilon J$. From the clear linear proportionality [Fig. 3(a)], one can unambiguously determine the constant ε. Interestingly, we find it to be essentially independent of V^* (or equivalently H^*), as is evident in Fig. 3(a).

The quadratic term cJ^2 is the next leading order contribution of J and thus negligible in the ideal limit $J \to 0$. However, the curvatures of the fitting curves in Fig. 2(b) indicate that the quadratic term is not completely negligible and the experimental data are somewhat above the ideal limit $J \to 0$. Thus, for a quantitative analysis of the J effect on the DW creep motion, one should take into

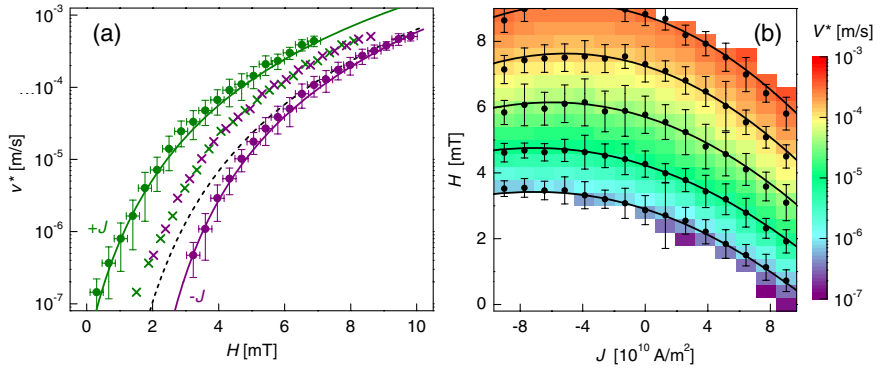

FIG. 2 (color online). (a) Relation between V^* and H for $J = \pm 7.7 \times 10^{10}$ A/m^2, respectively. The dotted line exhibits the pure FIDWM speed, identical to the best fit in Fig. 1(b). The cross symbols represent the horizontal middle points of the two curves, one for $+J$ and the other for $-J$. (b) Contour map of DW speed as a function of H and J.

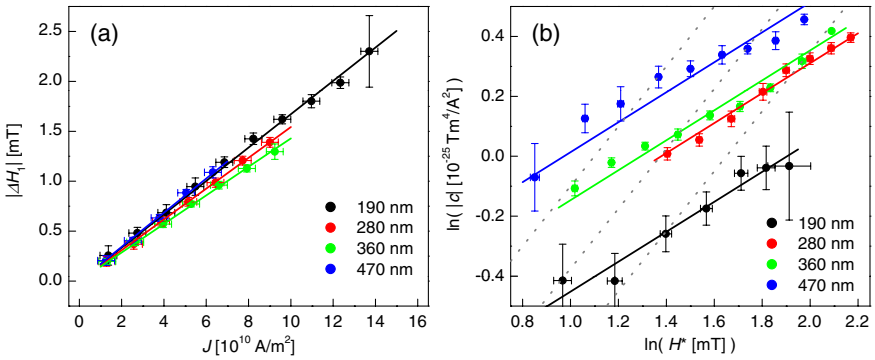

FIG. 3 (color online). The parameters measured for the nanowires with different widths. (a) $|\Delta H_1|$ vs J. The lines are the best linear fits. (b) The log-log scaling plot of $|c|$ with respect to H^*. The solid lines are the best linear fits with the slope $1/2$ and the dotted lines are guide for the slope 1.

account the *finite* J effect. Since the quadratic term boosts V^* regardless of the sign of J, one of its possible sources is the Joule heating. We believe that this is unlikely since the temperature rises by only several degrees [19] over the experimental range of J in Fig. 2(b), and also, this effect has been already compensated through the conversion from V to V^*. Moreover, if the Joule heating compensation was not satisfactory ($T_0 \rightarrow T_0 + \gamma J^2$ with γ representing the degree of unsatisfactory compensation), γ would generate an additive correction to $|c|$ proportional to H^* [dotted line in Fig. 3(b)]. In contrast, the experimental data indicate $|c| \propto \sqrt{H^*}$ [Fig. 3(b)]. This allows us to safely exclude the Joule heating possibility. Then the entire experimental data in Fig. 2(b) can be described by a single equation

$$H = H^* + \varepsilon J + \eta\sqrt{H^*}J^2, \tag{1}$$

where η is a constant independent of H^* [Fig. 3(b)]. For given H^*, Eq. (1) defines one equispeed contour line with the speed $V^* = V_0 \exp[-\alpha(H^*)^{-\mu}/k_B T_0]$.

A recent theory [20] analyzes the effect of the current-induced adiabatic and nonadiabatic STT on FIDWM. It predicts that the DW speed depends on H and J through a single variable $H^*_{\rm th}$; that is,

$$V^*(H, J) = V_0 \exp[-\alpha(H^*_{\rm th})^{-\mu}/k_B T_0], \tag{2}$$

where $H^*_{\rm th}$ is given by

$$H^*_{\rm th} = H - \varepsilon_{\rm th} J - \eta_{\rm th} J^2\sqrt{H - \varepsilon_{\rm th} J} + \frac{2}{5}\eta^2_{\rm th} J^4 + \cdots, \tag{3}$$

for small H and J. Here $\varepsilon_{\rm th}$ arises from the nonadiabatic STT and is thus proportional to the nonadiabaticity parameter β [13,15]. On the other hand, $\eta_{\rm th}$ is related to the adiabatic STT and is independent of β. After a simple algebra, Eq. (3) can be converted to an implicit form, $H = H^*_{\rm th} + \varepsilon_{\rm th} J + \eta_{\rm th}\sqrt{H^*_{\rm th}}J^2 + \cdots$, which is in complete agreement with Eq. (1). Thus, the nonadiabatic and adiabatic STT provide a natural explanation of the linear and quadratic terms in Eq. (1), respectively.

Next we examine pure CIDWM. In our nanowires, pure CIDWM is accomplished at $J < 10^{11}$ A/m^2 (260 μA in total current through the device). Figure 4(a) plots the pure CIDWM as a function of J. We first tried to fit the experimental data with a simple scaling curve $V^*(H = 0, J) = V_0 \exp[-\alpha'(J)^{-\mu'}/k_B T_0]$ with a number of different exponents μ' but always found systematic deviations. When μ' is regarded as a free parameter, the best fitting is achieved for $\mu' \simeq -1/2$, which is a nonphysical value since it implies a finite V^* for $J = 0$. This failure of the simple fitting curve indicates that the critical scaling regime of the pure CIDWM is very narrow and that one should take into

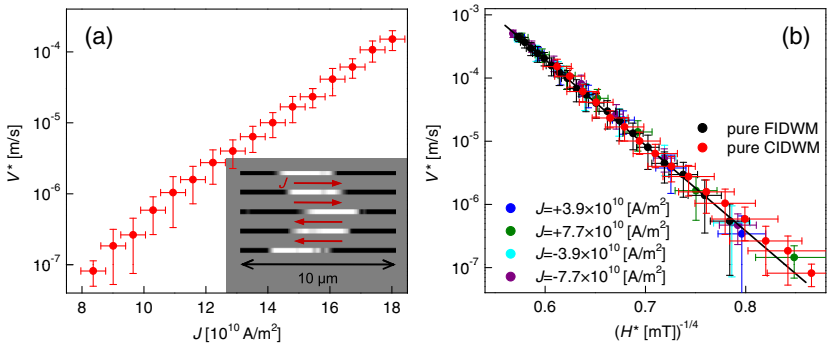

FIG. 4 (color online). (a) The pure CIDWM V^* vs J. Inset shows the motion of two DWs as a response to J. (b) V^* vs $(H^*)^{-1/4}$ for the DW motion driven by either pure H or J or both.

account corrections due to the finiteness of J in order to extract the information about the critical regime.

The theory [20] provides one testable prediction of the finite J effect. It predicts that if the nonadiabatic STT is dominant over the adiabatic STT, the pure CIDWM should also follow Eqs. (2) and (3) with the same exponent $\mu = 1/4$, and the leading corrections due to the finiteness of J are captured by the terms containing η_{th} in Eq. (3). Figure 4(b) provides an experimental test of the prediction. When J is converted to the effective driving force H^*, the data for the pure CIDWM (red symbols) form a straight line for the choice $\mu = 1/4$ and collapse onto the data for the pure FIDWM (black symbols), confirming that the theoretical prediction Eqs. (2) and (3) hold even for the pure CIDWM. Moreover, the data for both finite J and H also fall onto the same curve. Considering that the collapse onto the single universal curve is achieved by using only two fitting parameters, ε and η (below we drop the subscript ''th''), the collapse constitutes strong evidence that the pure CIDWM and FIDWM in Pt-Co-Pt nanowires belong to the same universality class.

A few remarks are in order. The inset of Fig. 4(a) shows the simultaneous motion of two DWs with different structures (black to white versus white to black). While the field drives the two DWs in the opposite directions, the STTs should drive them in the same direction. This difference leads to the prediction that the two DWs should have ε (and η) of equal magnitude but opposite signs. In agreement with this prediction of the STT theories, we find the fitting parameters $\varepsilon = \pm(1.6 \pm 0.1) \times 10^{-14}\ \mathrm{T\,m^2/A}$ and $\eta = \pm(1.8 \pm 0.2) \times 10^{-24}\ \mathrm{T^{1/2}\,m^4/A^2}$ for the two DWs.

The magnitude of ε is comparable to the nonadiabatic STT efficiency values reported by several experimental groups [17,21,22]. For various Co-Pt-based systems, however, the reported nonadiabatic STT efficiencies are widely dispersed between 0.2 and 8.0 times $10^{-14}\ \mathrm{T\,m^2/A}$. This may be due to the spin current polarization P, which is sensitive to the composition of Co and Pt [23]. According to the theory [20], ε is proportional to the nonadiabaticity parameter β, which leads to the estimation [22] $|\beta| \geq 0.38$. This value is comparable in magnitude to the Gilbert damping constant in Pt-Co-Pt films with a thin Co layer [24].

One peculiar feature of the experimental data is that the CIDWM occurs in the opposite direction of the charge carrier [25–27]. The Rashba spin-orbit coupling (RSOC) has been proposed as a possible origin of this effect for the case of strongly asymmetric layer structures Pt-Co-AlO_x [25,27]. However, we expect this effect to be much weaker in our samples since the upper and lower Pt layers have similar thickness and thus the effects from their interfaces tend to cancel each other. A recent theoretical analysis [20] addresses the RSOC effect perturbatively and finds that the RSOC correction to H^* is proportional to J^3 for the Bloch DW. Presently we do not have any clear experimental indication of the J^3 term, and experimental search for this effect requires the exploration of a higher current density regime, which goes beyond the scope of this Letter.

Our analysis indicates that the Oersted field from the current is irrelevant to the DW motion, since the two DWs move in the same direction irrespective of the magnetic polarities of the neighboring domains. The hydromagnetic drag and Hall charge effects [28] are estimated to be several orders smaller than our experimental data. Another possible origin is negative βP, since according to the STT theories [12,13] the STT-driven DW motion direction depends on the product βP. A recent band-based calculation of CoPt films [23] predicts the negative P for low Co concentration, which is consistent with our sample structure with a very thin Co layer sandwiched between much thicker Pt layers. A recent theory [29] also predicts that β can be negative. Presently we are unable to distinguish these two possibilities. Independent measurements of P and β are desired in future studies.

The earlier study [10] for (Ga,Mn)As reports different universality classes for FIDWM and CIDWM with the creep exponent $\mu \approx 1.2$ and 0.33, respectively. In contrast, for Pt-Co-Pt, the emergence of the single universal curve indicates that both the motions belong to the same universality class with the exponent $\mu = 1/4$. This establishes that, for the CIDWM, there are at least two different universality classes. One important element for multiple universality classes is the difference in the nature of the disorder (random-bond or random-field type) [9,10]. Another important element is the competition between the adiabatic and nonadiabatic STTs. This signals at the possibility of $2 \times 2 = 4$ different universality classes for the CIDWM. Our experimental data exemplify the dominance of the nonadiabatic STT in random-bond disorder while Ref. [10] reports the dominance of the adiabatic STT in random-field disorder.

A naturally occurring question is then the possibility of the third and fourth universality classes characterized by the remaining two combinations. Reference [30] predicts that, in a certain range of the nanowire width, the adiabatic STT rather than the nonadiabatic STT determines the threshold current density in metallic ferromagnetic nanowires with the perpendicular magnetic anisotropy. This prediction was recently verified [31], which provides a good candidate system for another universality class characterized by the dominance of the adiabatic STT in random-bond disorder. Furthermore, recalling that the DW motion is the coupled dynamics between the DW position and the DW tilting angle, the Walker breakdown [32] may be another important element for the universality classes and introduces additional factor two to the number of the universality classes. If all these combinations are possible, the number of the universality classes of the CIDWM increases to eight for the creep regime. Note

that another factor three would possibly be introduced with inclusion of the steady and turbulent flow regimes.

To conclude, it was demonstrated that the FIDWM and CIDWM belong to the same universality class in metallic ferromagnet Pt-Co-Pt, which is in clear contrast to semiconducting ferromagnet (Ga,Mn)As [10]. Analysis of the experimental data provides interesting future research directions such as multiple universality classes, DW motion in negative spin polarization, or negative nonadiabaticity materials. It also demands considerable advances in the statistical physics of the driven interface, theories [9] of which take account of disorder nature only but miss possible roles of multiple driving forces (adiabatic versus nonadiabatic STT) and additional degrees of freedom (DW tilting angle in addition to DW position).

This work was supported by NRF funded by MEST through Mid-career Researcher Program (2007-0056952, 2009-0084542, 2009-0083723, 2010-0014109) and SRC Program (2010-0001858). S. B. C. was supported by the SBS Foundation in Korea. J. C. L. and K. H. S. were supported by the KIST Institutional Program, by the KRCF DRC program, and by the IT R&D program of MKE/KEIT (2009-F-004-01).

*Present address: Institute for Chemical Research, Kyoto University, Gokasho, Uji, Kyoto 611-0011, Japan.
†hwl@postech.ac.kr
‡sugbong@snu.ac.kr

[1] T. Lux and M. Marchesi, Nature (London) **397**, 498 (1999).
[2] J. M. Carlson, J. S. Langer, and B. E. Shaw, Rev. Mod. Phys. **66**, 657 (1994).
[3] J. P. Sethna, K. A. Dahmen, and C. R. Myers, Nature (London) **410**, 242 (2001).
[4] B. Suki *et al.*, Nature (London) **368**, 615 (1994).
[5] G. Blatter *et al.*, Rev. Mod. Phys. **66**, 1125 (1994).
[6] K.-J. Kim *et al.*, Nature (London) **458**, 740 (2009).
[7] K.-S. Ryu, H. Akinaga, and S.-C. Shin, Nature Phys. **3**, 547 (2007).
[8] S. Lemerle *et al.*, Phys. Rev. Lett. **80**, 849 (1998).
[9] P. Chauve, T. Giamarchi, and P. LeDoussal, Phys. Rev. B **62**, 6241 (2000).
[10] M. Yamanouchi *et al.*, Science **317**, 1726 (2007).
[11] T. Nattermann, Y. Shapir, and I. Vilfan, Phys. Rev. B **42**, 8577 (1990).
[12] G. Tatara and H. Kohno, Phys. Rev. Lett. **92**, 086601 (2004).
[13] S. Zhang and Z. Li, Phys. Rev. Lett. **93**, 127204 (2004).
[14] R. A. Duine and C. M. Smith, Phys. Rev. B **77**, 094434 (2008).
[15] A. Thiaville *et al.*, Europhys. Lett. **69**, 990 (2005).
[16] M. Hayashi *et al.*, Phys. Rev. Lett. **98**, 037204 (2007).
[17] L. San Emeterio Alvarez *et al.*, Phys. Rev. Lett. **104**, 137205 (2010).
[18] J. Kim, K.-J. Kim, and S.-B. Choe, IEEE Trans. Magn. **45**, 3909 (2009).
[19] K.-J. Kim *et al.*, Appl. Phys. Lett. **92**, 192509 (2008).
[20] J. Ryu, S.-B. Choe, and H.-W. Lee, arXiv:1104.0744 [Phys. Rev. B (to be published)].
[21] I. M. Miron *et al.*, Phys. Rev. Lett. **102**, 137202 (2009).
[22] O. Boulle *et al.*, Phys. Rev. Lett. **101**, 216601 (2008).
[23] O. Šipr *et al.*, Phys. Rev. B **78**, 144403 (2008).
[24] S. Mizukami *et al.*, Appl. Phys. Lett. **96**, 152502 (2010).
[25] I. M. Miron *et al.*, Nature Mater. **10**, 419 (2011).
[26] M. Yamanouchi *et al.*, Phys. Rev. Lett. **96**, 096601 (2006).
[27] T. A. Moore *et al.*, Appl. Phys. Lett. **95**, 179902 (2009).
[28] M. Viret *et al.*, Phys. Rev. B **72**, 140403(R) (2005).
[29] S. Bohlens and D. Pfannkuche, Phys. Rev. Lett. **105**, 177201 (2010).
[30] S.-W. Jung *et al.*, Appl. Phys. Lett. **92**, 202508 (2008).
[31] T. Koyama *et al.*, Nature Mater. **10**, 194 (2011).
[32] G. S. D. Beach *et al.*, Nature Mater. **4**, 741 (2005).